INTERNATIONAL JOURNAL OF
NUMERICAL ANALYSIS AND MODELING
Volume 11, Number 2, Pages 372–384

RECENT ADVANCES ON EXPLICIT VARIATIONAL MULTISCALE A POSTERIORI ERROR ESTIMATION FOR SYSTEMS

GUILLERMO HAUKE, DIEGO IRISARRI, AND FERNANDO LIZARRAGA

(Communicated by R. Celorrio)

This paper is dedicated to F. Lisbona

Abstract. In 1995 the genesis of stabilized methods was established by Professor Hughes from the standpoint of the variational multiscale theory (VMS). By splitting the solution into *resolved* and *unresolved* scales, it was unveiled that stabilized methods take into account an approximation of the *unresolved* scales or *error* into the finite element solution. In this work, the VMS theory is exploited to formulate an explicit a-posteriori error estimator, consistent with the assumptions inherent to stabilized methods.The proposed technology, which is especially suited for fluid flow problems, is very economical and can be implemented in standard finite element codes. It has been shown that, in practice, the method is robust uniformly from the diffusive to the hyperbolic limit.The success of the method can be explained by the fact that in stabilized methods the element local problems for the fine-scale Green's function capture most of the error and the error intrinsic time-scales are an approximation to the solution of the dual problem. Applications to the Euler and linear elasticity equations are shown.

Key words. A posteriori error estimation, stabilized methods.

1. Introduction

The main objective of numerical methods is to obtain reliable approximate solutions. One way of achieving this goal is by quantifying the error and generating adaptive meshes which distribute the error of the numerical solution within the problem domain [1, 2]. This paper summarizes current research on *explicit* a posteriori error estimation for stabilized methods based on the variational multiscale theory (VMS) [25, 27]. This theory is especially suited for estabilized methods and fluid mechanics problems, but it also may find application in solid mechanics.

Within the VMS framework, the first explicit a posteriori error estimator was proposed for the transport equation in [17]. This formulation is a residual-based error estimator and, therefore, the error in each element is estimated as a function of the residual inside the element. There, the capabilities to generate adapted meshes were shown. The resulting method fits in the framework of residual-based methods proposed in [31, 32] but, here, the constants of the error estimates, which are dimensionally consistent, are explicitly given by the theory.

Further achievements on the technology for the transport equation were presented in [13, 17, 18]. Later, the error estimator was extended for the multi-dimensional transport equation in [20], where the jump of the flux along the element edges must be taken into account to attain reliable error estimates in the diffusive dominated

Received by the editors November 1, 2012 and, in revised form, April 11, 2013.
2000 *Mathematics Subject Classification.* 35Q31.
This research was partly supported by the Ministry of Science and Technology of Spain under grant number MTM2010-20463, Spanish MECD under FPU grant (AP210-2073), Departamento de Industria e Innovación del Gobierno de Aragón and the European Social Fund.

regime. These estimators have been tested with practical cases attaining reliable and robust results. All these findings are summarized in [15].

Subsequently, the a posteriori error estimator was extended to the topic of quantities of interest in [19] and to higher-order finite elements [28, 16].

For elliptic problems other methods based on the VMS theory are those of [7, 8, 30, 29]. But in these, the subscales are computed at the element level with the corresponding partial differential equations.

The next challenge consists of extending the present technology to systems of equations. Thus, this paper presents recent advances in relation to the Euler equation and linear elasticity. The error estimator formulation and practical examples are explained in this paper.

2. VMS theory. Error estimation

2.1. The abstract problem. Let Ω be a spatial domain with boundary Γ. The boundary is partitioned into two non-overlapping zones Γ_g and Γ_h such that $\Gamma_g \cup \Gamma_h = \Gamma$ and $\Gamma_g \cap \Gamma_h = \oslash$. The essential boundary condition g is applied on Γ_g and the natural boundary condition, h, on Γ_h.

The strong form of the boundary-value problem consists of finding $u : \Omega \to \mathbb{R}$ such that for the given functions $f : \Omega \to \mathbb{R}$, $g : \Gamma_g \to \mathbb{R}$, $h : \Gamma_h \to \mathbb{R}$, the following equations are satisfied

$$\left\{ \begin{array}{rcll} \mathcal{L}u & = & f & \text{in } \Omega \\ u & = & g & \text{on } \Gamma_g \\ \mathcal{B}u & = & h & \text{on } \Gamma_h \end{array} \right. \tag{1}$$

with $\mathcal{L}$ being a general differential operator and $\mathcal{B}$, an operator acting on the boundary emanating from integration-by-parts.

In order to introduce the weak form, we have to define suitable spaces for the trial solution, $\mathcal{S}$, and the weighting functions $\mathcal{V}$. The weak form is obtained by multiplying the strong form equation by a weighting function, w, and integrating by parts. Hence, the weak form can be formulated as:

Find $u \in \mathcal{S}$ such that

$$a(w,u) = (w,f) + (w,h)_{\Gamma_h} \qquad \forall w \in \mathcal{V} \tag{2}$$

where $a(\cdot,\cdot)$ is the corresponding bilinear form; $(\cdot,\cdot)$ the $L_2(\Omega)$ inner product and $(\cdot,\cdot)_{\Gamma_h}$, the $L_2(\Gamma_h)$ inner product on Γ_h.

Application of the finite element method necessitates the discretization of the domain Ω into n_{el} non-overlapping elements with domain Ω^e and boundary Γ^e. Let $\widetilde{\Omega}$ and $\widetilde{\Gamma}$ denote the union of element interiors and the inter-element boundaries, respectively,

$$\begin{aligned} \widetilde{\Omega} &= \bigcup_{e=1}^{n_{\text{el}}} \Omega^e \\ \widetilde{\Gamma} &= \bigcup_{e=1}^{n_{\text{el}}} \Gamma^e \backslash \Gamma \end{aligned} \tag{3}$$

In addition, let $[\![\cdot]\!]$ be the jump operator of a function across a discontinuity, for example, an inter-element boundary. According to Fig. 1, the jump of a function

$\boldsymbol{v} \cdot \boldsymbol{n}$ is defined as

$$[\![\boldsymbol{v} \cdot \boldsymbol{n}]\!] = \boldsymbol{v}^+ \cdot \boldsymbol{n}^+ + \boldsymbol{v}^- \cdot \boldsymbol{n}^- \tag{4}$$

where $\boldsymbol{n}$ is the outward unit normal vector.

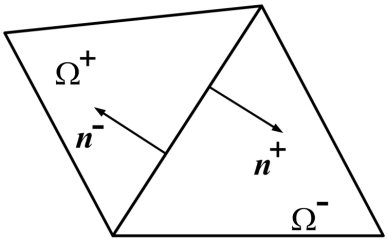

FIGURE 1. Notation to define the jump across element interfaces

2.2. The multiscale approach. Following the variational multiscale theory [25, 27], the solution and weighting functions are decomposed into resolved and unresolved scales,

$$\begin{array}{lll} u = \overline{u} + u' & \overline{u} \in \overline{\mathcal{S}} & u' \in \mathcal{S}' \\ w = \overline{w} + w' & \overline{w} \in \overline{\mathcal{S}} & w' \in \mathcal{S}' \end{array}$$

where u is the exact solution, $\bar{u}$, the finite element solution (resolved scales), u', the error (unresolved scales). The spaces are defined such that $\mathcal{S} = \bar{\mathcal{S}} \oplus \mathcal{S}'$ and $\mathcal{V} = \bar{\mathcal{V}} \oplus \mathcal{V}'$.

Thanks to the bilinearity of $a(\cdot, \cdot)$, the above variational formulation can be decomposed into two subproblems

$$\begin{array}{ll} a(\bar{w}, \bar{u} + u') & = (\bar{w}, f) + (\bar{w}, h)_{\Gamma_h} \\ a(w', \bar{u} + u') & = (w', f) + (w', h)_{\Gamma_h} \end{array} \tag{5}$$

The first equation of (5) is related to the resolved scales or coarse scales of the solution, $\bar{u}$, and the second one, to the unresolved scales or fine scales, u', [25, 27].

In this work, the fine scales are solved by means of a Green's function $g'(x, y)$, the so-called *fine-scale* Green's function [28]. Given two points $x, y \in \Omega$, these scales are exactly given by

$$\begin{aligned} u'(x) = & -\int_{\widetilde{\Omega}} g'(x,y)(\mathcal{L}\bar{u} - f)(y)\, \mathrm{d}\Omega_y \\ & -\int_{\widetilde{\Gamma}} g'(x,y)([\![\mathcal{B}\bar{u}]\!])(y)\, \mathrm{d}\Gamma_y \\ & -\int_{\Gamma_h} g'(x,y)\ (\mathcal{B}\bar{u} - h)(y)\, \mathrm{d}\Gamma_y \end{aligned} \tag{6}$$

Thus, $u'(x)$ can be used to estimate the error of $\bar{u}$.

The error estimator is residual based and the contemplated residuals include:

- Element interior residuals, $\mathcal{L}\bar{u} - f$ in $\widetilde{\Omega}$
- Inter-element residuals, $[\![\mathcal{B}\bar{u}]\!]$ on $\widetilde{\Gamma}$
- Natural boundary condition residual, $\mathcal{B}\bar{u} - h$ on Γ_h

As can be seen, we only need the finite element solution to estimate the error. Generally speaking, the computation of Eq. (6) can become complex depending on the analyzed problem. Mainly, the difficulties might appear when we have to obtain the Green's function for the fine scale problem, $g'(x,y)$, and when we have to compute the convolution integrals which are non-local.

2.3. Error estimation paradigm.

2.3.1. Smooth paradigm. In many cases, some simplifications can be made so as to make easier the calculus of Eq. (6). If $\bar{u}$ is exact on Γ^e, the boundary integrals vanish and the error decouples from element to element. In addition, it is possible to replace the fine-scale Green's function with the element Green's function $g_e(x,y)$ [17], which can be obtained as the solution of the following problem

$$\left\{ \begin{array}{rll} \mathcal{L}g_e &= \delta_y & \text{in} \quad \Omega^e \\ g_e &= 0 & \text{on} \quad \Gamma^e \end{array} \right.$$

where $\delta_y(x) = \delta(x-y)$ is the Dirac's delta function.

Therefore, in this context the error in each element Ω^e depends only on residuals inside the element. That is, the error estimator becomes

$$u'(x) = -\int_{\Omega^e} g_e(x,y)\ (\mathcal{L}\bar{u} - f)(y)\ \mathrm{d}\Omega_y \qquad \text{on } \Omega^e \tag{7}$$

If the residual is constant inside the element, i.e., $(\mathcal{L}\bar{u} - f) \in \mathcal{P}_0$, Eq. (7) reveals that

$$\begin{aligned} u'(x)|_{\Omega^e} &= -\int_{\Omega_e} g_e(x,y)(\mathcal{L}\bar{u} - f)(y)\ \mathrm{d}\Omega_y \\ &= -(\mathcal{L}\bar{u} - f)\int_{\Omega_e} g_e(x,y)\ \mathrm{d}\Omega_y \\ &= -(\mathcal{L}\bar{u} - f)\ b_0^e(x) \end{aligned} \tag{8}$$

where $b_0^e(x) = \int_{\Omega_e} g_e(x,y)\ \mathrm{d}\Omega_y$ is a *residual-free* bubble function [4, 6, 5, 17], also solution of the problem

$$\left\{ \begin{array}{rll} \mathcal{L}b_0^e &= 1 & \text{in} \quad \Omega^e \\ b_0^e &= 0 & \text{on} \quad \Gamma^e \end{array} \right. \tag{9}$$

In relation to the bubble function, we define the *error scale*, $\tau_{L_r}^e$, which is an average of the local Green's function

$$\boxed{\tau_{L_r}^e = \frac{1}{\mathrm{meas}(\Omega^e)^{1/r}}\ ||b_0^e(x)||_{L_r(\Omega^e)}} \tag{10}$$

For the transport equation, this parameter has dimensions of time and it becomes an *error time-scale* as the *flow* stabilization parameter employed to stabilize the Galerkin method in stabilized methods [25].

2.3.2. Multidimensional case. The assumption that $\bar{u}$ is exact on Γ^e might not be suitable for multi-dimensional problems. The error, in these cases, might be non-local. The strategy for the multidimensional setting consists of decomposing the error into two parts, one related to the element interior residual, $u'_{\mathrm{int}}(x)$, and the other one related to the inter-element residual, $u'_{\mathrm{bnd}}(x)$,

$$u'(x) = u'_{\mathrm{int}}(x) + u'_{\mathrm{bnd}}(x) \tag{11}$$

By the triangle inequality

$$||u'(x)|| \leq ||u'_{\text{int}}(x)|| + ||u'_{\text{bnd}}(x)|| \tag{12}$$

The term $u'_{\text{bnd}}(x)$ is connected to the non-smooth derivatives across the element boundaries of the finite element solution, $\bar{u}$. Assuming the method presents a mostly local error distribution, we describe both $u'_{\text{int}}(x)$ and $u'_{\text{bnd}}(x)$ as

$$u'_{\text{int}}(x) \approx -\int_{\Omega^e} g_e(x,y)\ (\mathcal{L}\bar{u} - f)(y)\ d\Omega_y \qquad \text{on } \Omega^e \tag{13}$$

and

$$u'_{\text{bnd}}(x) \approx -\int_{\Gamma^e} g'(x,y)\ ([\![\mathcal{B}\bar{u}]\!])(y)\ d\Gamma_y \qquad \text{on } \Omega^e \tag{14}$$

Applying Hölder's inequality [3] ($1 \leq p, q \leq \infty$, $1/p + 1/q = 1$)

$$|u'_{\text{int}}(x)| \leq ||g_e(x,y)||_{L_p(\Omega^e_y)}\ ||\mathcal{L}\bar{u} - f||_{L_q(\Omega^e)}$$

$$|u'_{\text{bnd}}(x)| \leq ||g'(x,y)||_{L_p(\Gamma^e_y)}\ ||[\![\mathcal{B}\bar{u}]\!]||_{L_q(\Gamma^e)}$$

Finally, taking the L_r norm

$$||u'_{\text{int}}(x)||_{L_r(\Omega^e)} \leq \Big|\Big|\ ||g_e(x,y)||_{L_p(\Omega^e_y)}\Big|\Big|_{L_r(\Omega^e_x)}\ ||\mathcal{L}\bar{u} - f||_{L_q(\Omega^e)} \tag{15}$$

$$||u'_{\text{bnd}}(x)||_{L_r(\Omega^e)} \leq \Big|\Big|\ ||g'(x,y)||_{L_p(\Gamma^e_y)}\Big|\Big|_{L_r(\Omega^e_x)} \tag{16}$$

To sum up, for $p = 1$ and $q = \infty$ the general formulation employed to obtain a measure of the error is the following expression [20]

$$\boxed{\begin{aligned} ||u'(x)||_{L_r(\Omega^e)} \ &\leq\ \text{meas}(\Omega^e)^{1/r}\ \tau^e_{L_r} \\ &\times \left(||\mathcal{L}\bar{u} - f||_{L_\infty(\Omega^e)} + \tfrac{1}{2}\frac{\text{meas}(\Gamma^e)}{\text{meas}(\Omega^e)}\right) \quad \text{on } \Omega^e \end{aligned}} \tag{17}$$

3. Previous results

Let us begin by recalling previous results on VMS a posteriori error estimation. Mainly, they are results where the models are applied to the transport equation. Satisfactory results are achieved for a wide range of Peclet numbers both in one-dimension and in multi-dimensions.

A way of evaluating the quality of the error estimator is to relate the predicted error η and the true error. The local effectivity in each element is defined as

$$I^e_{\text{eff}} = \frac{||\text{Predicted error}||}{||\text{True error}||} = \frac{||\eta^e||}{||\bar{u} - u||_{\Omega^e}} \tag{18}$$

The global effectivity, depending on the norm L_r, is given by

$$I^G_{\text{eff},L_r} = \left(\frac{\sum_{e=1}^{n_{\text{el}}} (\eta^e)^r}{\sum_{e=1}^{n_{\text{el}}} ||\bar{u} - u||^r_{\Omega^e}}\right)^{1/r} \tag{19}$$

3.1. 1-D Models. The above concepts on a posteriori error estimation were applied to 1D advection-diffusion-reaction problems, where $\mathcal{L}u = au_{,x} - \kappa u_{,xx} - su$, with a the fluid velocity, κ the diffusivity and s a source parameter [13, 18]. Fig. 2 shows the error time-scale $\tau^e_{L_2}$ as a function of the element Peclet number $\alpha = |a|h^e/(2\kappa)$, where h^e is the element length. The behavior of the error time-scale is very similar to that of the stabilization parameter τ^e_{flow}.

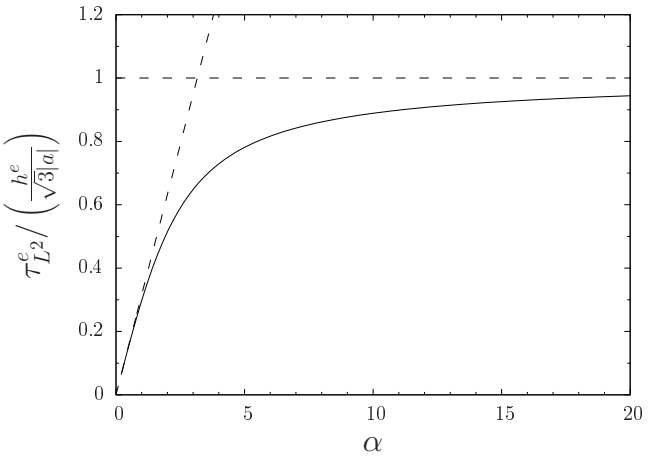

FIGURE 2. One-dimensional advection-difussion problem. Exact and asymptotic dimensionless error time-scale $\tau^e_{L_2}$ as a function of the element Peclet number α

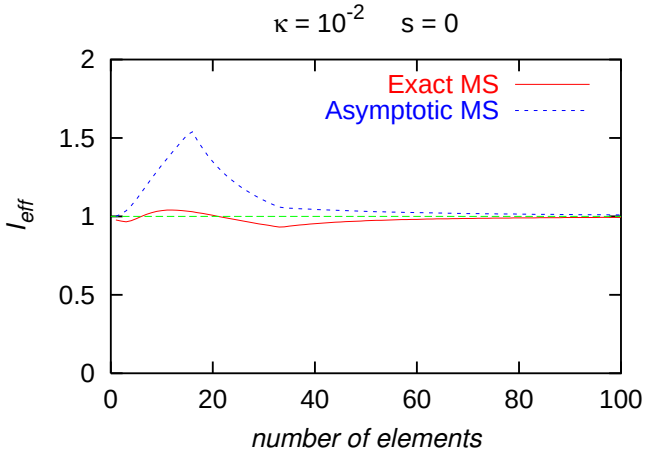

FIGURE 3. Global effectivity index for one dimensional advection-diffusion. "Exact MS" shows the results employing the exact expression for the error time-scale and "Asymptotic MS," the results using the asymptotic approximation depicted in Fig. 2

The technology is really successful for element Peclet numbers ranging from the diffusion dominated regime till the advection dominated regime. This is illustrated

in Fig. 3, where the global effectivity index is shown as a function of the number of elements. As can be appreciated, the predicted error is very accurate, especially when the number of elements is increased. The finite element solution is computed with the SGS stabilized method [9, 10, 11].

3.2. Multi-dimensional Model. The above ideas have been extended to multi-dimensional transport problems in [14, 20]. It was shown that in the multi-dimensional setting it is necessary to involve the inter-element boundary error in the diffusion dominated regime because the finite element solution is not exact along the element edges.

As mentioned before, it is possible to create adaptive strategies in order to adjust the mesh size in the problem domain and, thus, optimize the computational time. Given an error tolerance, $e_{\text{tol}} = ||u - \bar{u}||_{\Omega^e} = ||u'_{\text{tol}}||_{\Omega^e}$, the local norm of the estimated error $\eta_{L_2}^{e(i)} \approx ||u'||_{\Omega^e}$ at iteration (i), and the mesh size distribution $h^{e(i)}$ at iteration (i), it can be shown that the new mesh size distribution at iteration $(i+1)$ is

$$h^{e(i+1)} = \left[\frac{e_{\text{tol}}}{\eta_{L_2}^{e(i)}}\right]^{1/p} h^{e(i)} \tag{20}$$

with p the order of convergence of the solution. In our case, although more efficient strategies are available using coarsening and refining algorithms, at each iteration the mesh is regenerated using a commercial mesh generator. For other norms and remeshing strategies, the interested reader is referred to [12].

The L-shaped problem is a common benchmark applied to the transport equation. The image on the left of Fig. 4 illustrates the initial mesh of the problem whereas the image on the right shows the adaptive mesh, where the size of the elements is reduced inside the boundary, outflow and interior layers.

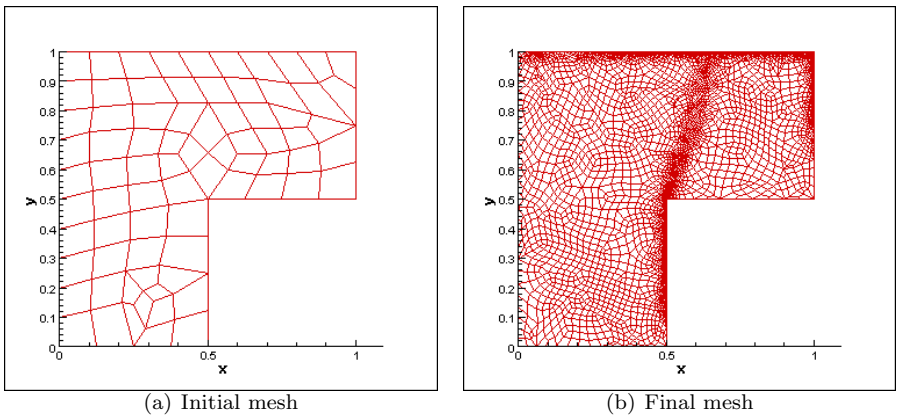

(a) Initial mesh (b) Final mesh

FIGURE 4. Adaptativity in FEM meshes in L-shaped problem

4. Application to systems. Recent advances

An interesting extension of the above concepts is to investigate the effectivity of the previous models when applied to systems. Recent research has been developed in relation to the Euler equations and linear elasticity.

When we face these models, new challenges and difficulties emerge. For instance, there is not only a single unknown but many variables appear in the finite element method formulation. Furthermore, in fluid mechanics the system of partial differential equations is nonlinear.

4.1. Error estimation models. The general strong form is as follows.

Find $\mathbf{Y} : \Omega \to \mathbb{R}^{n_{\text{eq}}}$ such that

$$\left\{ \begin{array}{rcll} \boldsymbol{\mathcal{L}}\mathbf{Y} & = \mathbf{0} & \text{in} & \Omega \\ \mathbf{Y} & = \boldsymbol{\mathcal{G}} & \text{on} & \Gamma_{\mathcal{G}} \\ \boldsymbol{\mathcal{B}}\mathbf{Y} & = \boldsymbol{\mathcal{H}} & \text{on} & \Gamma_{\mathcal{H}} \end{array} \right. \tag{21}$$

where

$$\begin{aligned} \boldsymbol{\mathcal{L}}\mathbf{Y} &= \mathbf{A}_i \mathbf{Y}_{,i} + (\mathbf{K}_{ij}\mathbf{Y}_{,j})_{,j} - \mathbf{S} \\ &= \mathbf{F}^{\text{adv}}_{i,i} - \mathbf{F}^{\text{diff}}_{i,i} - \mathbf{S} \end{aligned} \tag{22}$$

contains, in the general case, the advection, diffusion and source term. The unknown term $\mathbf{Y}$ is a vector.

In the same way as Eq. (6), for linear systems the unresolved scales can be expressed as

$$\begin{aligned} \mathbf{Y}'(\mathbf{x}) = \quad & -\int_{\widetilde{\Omega}} \mathbf{G}'(\mathbf{x},\mathbf{y})\ (\boldsymbol{\mathcal{L}}\overline{\mathbf{Y}} - \overline{\mathbf{S}})(\mathbf{y})\ \mathrm{d}\Omega_y \\ & -\int_{\widetilde{\Gamma}} \mathbf{G}'(\mathbf{x},\mathbf{y})\ (\llbracket \boldsymbol{\mathcal{B}}\overline{\mathbf{Y}} \rrbracket)(\mathbf{y})\ \mathrm{d}\Gamma_y \\ & -\int_{\Gamma_{\mathcal{H}}} \mathbf{G}'(\mathbf{x},\mathbf{y})\ (\boldsymbol{\mathcal{B}}\overline{\mathbf{Y}} - \boldsymbol{\mathcal{H}})(\mathbf{y})\ \mathrm{d}\Gamma_y \end{aligned} \tag{23}$$

where $\mathbf{G}'(\mathbf{x},\mathbf{y})$ is the fine-scale Green's tensor.

4.2. Euler equations. Research about error estimation for the Euler equations has been carried on supersonic and subsonic flows [21]. A major difference in comparison with the above problems is the nonlinearity of the differential equation. The strong formulation of the problem is:

$$\left\{ \begin{array}{c} \dfrac{\partial \rho}{\partial t} + \nabla \cdot (\rho \boldsymbol{u}) = 0 \\ \dfrac{\partial \rho \boldsymbol{u}}{\partial t} + \nabla \cdot (\rho \boldsymbol{u}\boldsymbol{u}) + \nabla p = 0 \\ \dfrac{\partial \rho (E + \boldsymbol{u}\cdot\boldsymbol{u}/2)}{\partial t} + \nabla \cdot \left(\rho \boldsymbol{u} E + \rho \boldsymbol{u} \dfrac{\boldsymbol{u}\cdot\boldsymbol{u}}{2} + \boldsymbol{u} p \right) = 0 \end{array} \right. \tag{24}$$

where ρ is the density, $\boldsymbol{u}$ is the speed and p, the pressure, while E is the specific internal energy which can be determined via the corresponding equation of state.

The following expression gives an approximation of the error upper bound:

$$\boxed{\|Y_i'(\mathbf{x})\|_{L_r(\Omega_e)} \approx \text{meas}(\Omega_e)^{1/r} |\tau_{L_r ij}| \times \|(\boldsymbol{\mathcal{L}}\overline{\mathbf{Y}})_j\|_{L_\infty(\Omega_e)}} \tag{25}$$

The error estimator is applied to the subsonic flow around a symmetric Joukowski airfoil at a Mach number of 0.1, which has been solved with the stabilized method [22, 23] based on pressure-primitive variables. Fig. 5 and 6 depict the frequency distribution of the element efficiency for the velocity components and the pressure.

Fig. 7 shows an example of adapted mesh generated using the proposed error estimator.

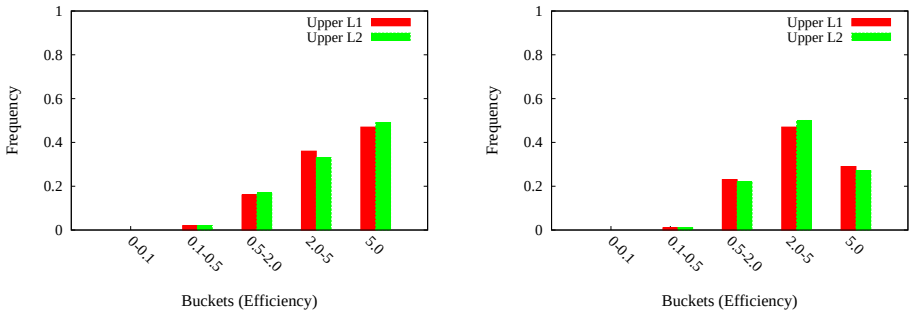

(a) Horizontal velocity component (b) Vertical velocity component

FIGURE 5. Joukowski airfoil problem. Frequency distribution for the horizontal velocity component and the vertical velocity component

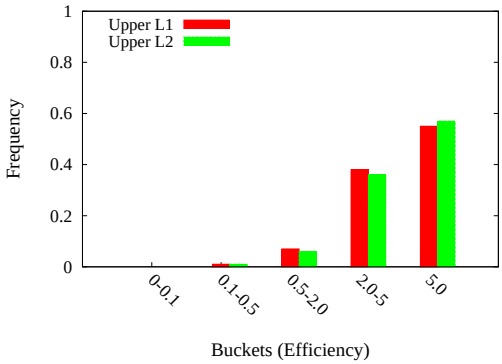

FIGURE 6. Joukowski airfoil problem. Frequency distribution for pressure

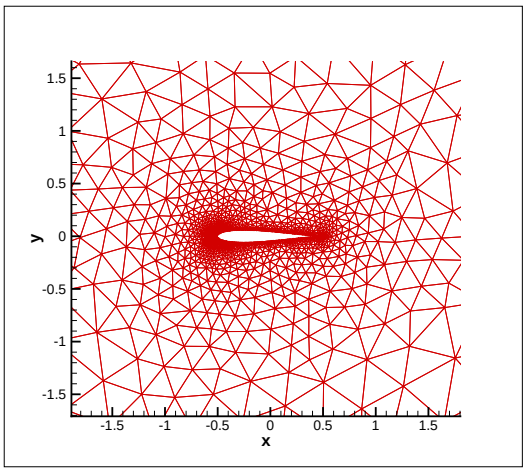

FIGURE 7. Joukowski airfoil problem. Adapted mesh

4.3. Linear elasticity. For linear elasticity, the error estimator has been developed for the energy norm. Error estimations based on L_r norms do not yield satisfactory results because the estimate gives a lower bound of the true error. This estimator has been applied to plane stress problems. The equilibrium equations for linear elasticity are given by

$$\left\{\begin{array}{rrll} \nabla\cdot\ \boldsymbol{\sigma}+\boldsymbol{f} & =\mathbf{0} & \text{in} & \Omega \\ \boldsymbol{u} & =\boldsymbol{g} & \text{on} & \Gamma_g \\ \boldsymbol{\sigma}\cdot\boldsymbol{n} & =\boldsymbol{h} & \text{on} & \Gamma_h \end{array}\right. \tag{26}$$

where $\boldsymbol{\sigma}$ is stress tensor; $\boldsymbol{f}$, the body force; $\boldsymbol{u}$, the unknown displacement vector; $\boldsymbol{g}$, the essential boundary condition and $\boldsymbol{h}$, the natural boundary condition. The stress tensor for plane stress is defined in indicial notation by

$$\sigma_{ij}=\lambda\varepsilon_{kk}\delta_{ij}+2G\varepsilon_{ij} \tag{27}$$

with λ and G being the Lamé parameters and $\boldsymbol{\varepsilon}$, the strain tensor which is expressed as $\varepsilon_{ij}=\frac{1}{2}(u_{i,j}+u_{j,i})$.

Following the above concepts, the error estimator is defined as [24]

$$\begin{aligned} ||\boldsymbol{u}'_{i,x}(\boldsymbol{x})||_{L_2(\Omega^e)} \ &\leq\ \text{meas}(\Omega^e)^{1/r}\tau^e_{H_1\,ij}\times \\ &\times\left(||(\boldsymbol{\mathcal{L}u}-\boldsymbol{f})_j||_{L_\infty(\Omega^e)}+\right. \\ &\left.+\tfrac{1}{2}\frac{\text{meas}(\Gamma^e)}{\text{meas}(\Omega^e)}||[\![\boldsymbol{\mathcal{B}}\bar{\boldsymbol{u}}]\!]_j||_{L_\infty(\Gamma^e)}\right)\text{on }\Omega^e \end{aligned} \tag{28}$$

with $\tau^e_{H_1\,ij}$, the scale to estimate the error in the derivative.

An example of plane stress is the L-shaped problem of Fig. 8 [33, 34], where we can see the loads, constraints and the finite element solution based on bilinear quadrilateral elements and the Galerkin method [26]. Once the finite element

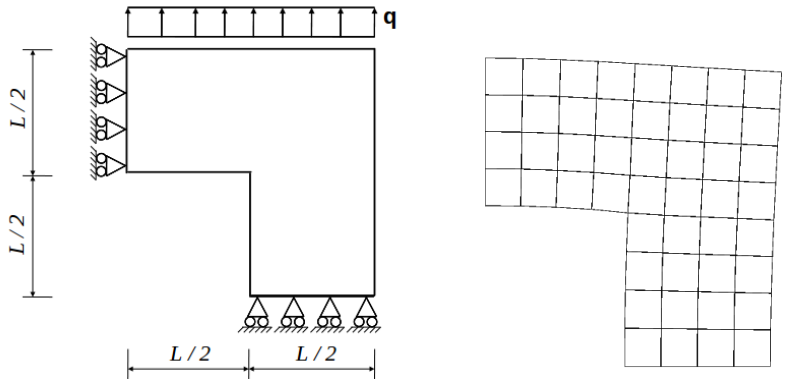

FIGURE 8. L-shaped problem. Setup

solution has been obtained, the error estimator (28) is applied. Local and global effectivities are depicted in Fig. 9, which additional illustrates the frequency distribution of the element effectivities.

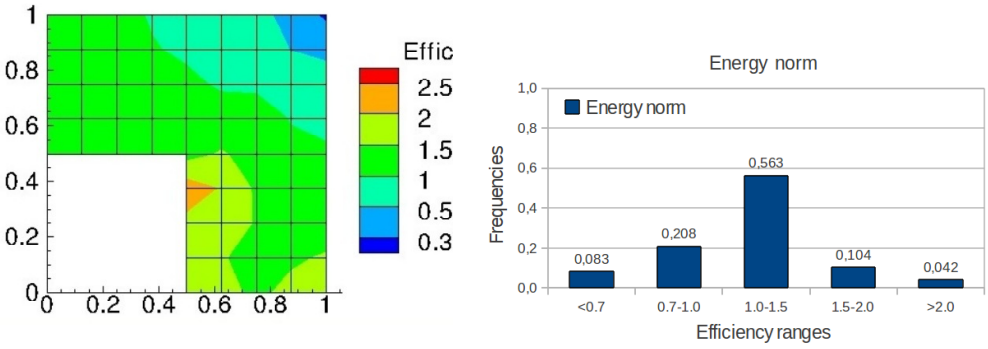

FIGURE 9. Local effectivitites for the L-shaped problem. Spatial distribution and frequency distribution

5. Conclusions

An explicit a posteriori error estimator based on the variational multiscale theory has been presented for different physical phenomena, in particular, the Euler equations and linear elasticity. It can be used to evaluate the quality of the finite element solution or to generate adapted meshes. The main advantages of this error estimator are that it is a very economical method and easy to implement in finite element method codes.

For the Euler equations, the estimates in the L_1 and L_2 norms work fairly well. In subsonic flows, for a precise error estimation, the error-time scales have to be based on a proper low Mach number stabilization matrix.

As regards linear elasticity, error estimates based on the L_r-norm give a lower bound of the error. However, the error estimates based on the H_1-norm yield successful results. This can be explained by the fact that that the error distribution in H_1-norm is more local than in L_r-norms. Let us recall that the Galerkin method is H_1 optimal.

The success of this estimator can be explained by the fact that it solves the local dual problems at the element level and since the error distribution is practically local, these represent fairly well the exact error. Moreover, the proposed technology achieves similar accuracy as implicit methods with less computational cost, since it is not necessary to solve any differential equation to calculate the error.

References

[1] Ainsworth, M., Oden, J.T.: A posterior error estimation in finite element analysis. John Wiley & Sons (2000)
[2] Bangerth, W., Rannacher, R.: Adaptive finite element methods for differential equations. Birkhäuser (2003)
[3] Brenner, S., Scott, L.: The mathematical theory of finite element methods. Springer-Verlag (2002)
[4] Brezzi, F., Bristeau, M., Franca, L.P., Mallet, M., Rogé, G.: A relationship between stabilized finite element methods and the galerkin method with bubble functions. Comput. Meth. Appl. Mech. Engrg. **96**, 117–129 (1992)
[5] Brezzi, F., Franca, L., Hughes, T., Russo, A.: $b = \int g$. Comput. Meth. Appl. Mech. Engrng. **145**, 329–339 (1997)
[6] Brezzi, F., Russo, A.: Choosing bubbles for advection-diffusion problems. Mathematical Models and Methods in Applied Sciences **4**, 571–587 (1994)

[7] ElSheik, A., Chidiac, S., Smith, W.: A posteriori error estimation based on numerical realization of the variational multiscale method. Comput. Meth. Appl. Mech. Engrg. **197**, 3637–3656 (2008)
[8] ElSheik, A., Smith, S., Chidiac, S.: Numerical investigation of the reliability of a posteriori error estimation for advection-diffusion equations. Commun. Numer. Meth. Engng. **24**, 711–726 (2008)
[9] Franca, L., Frey, S., Hughes, T.: Stabilized finite element methods: I. application to the advective-diffusive model. Comput. Meth. Appl. Mech. Engrng. **95**, 253–276 (1992)
[10] Franca, L., Valentin, F.: On an improved unusual stabilized finite element method for the advective-reactive-diffusive equation. Comput. Meth. Appl. Mech. Engrng. **190**, 1785–1800 (2000)
[11] Hauke, G.: A simple stabilized method for the advection-diffusion-reaction equation. Comput. Meth. Appl. Mech. Engrng. **191**, 2925–2947 (2002)
[12] Hauke, G., Doweidar, M., Fuentes, S.: Mesh adaptivity for the transport equation led by variational multiscale error estimators. Int. J. Num. Meth. Fluids **69**, 1835–1959 (2012)
[13] Hauke, G., Doweidar, M.H.: Intrinsic scales and a posteriori multiscale error estimation for piecewise-linear functions and residuals. Int. J. Comput. Fluid Dynamics **20**, 211–222 (2006)
[14] Hauke, G., Doweidar, M.H., Fuster, D.: Multiscale multi-dimensional explicit a-posteriori error estimation for fluid dynamics. In: P. Wesseling, E. Oñate, J. Périaux (eds.) European Conference on Computational Fluid Dynamics, pp. 1–13 (2006)
[15] Hauke, G., Doweidar, M.H., Fuster, D.: A posteriori error estimation for computational fluid dynamics. The variational multiscale approach. In: E. Ramm, R. de Borst (eds.) Multiscale Methods in Computational Mechanics, *Lecture Notes in Applied and Computational Mechanics*, vol. 55. Springer (2010)
[16] Hauke, G., Doweidar, M.H., Fuster, D., Gomez, A., Sayas, J.: Application of variational a-posteriori multiscale error estimation to higher-order elements. Computational Mechanics **38**, 382–389 (2006)
[17] Hauke, G., Doweidar, M.H., Miana, M.: The multiscale approach to error estimation and adaptivity. Comput. Meth. Appl. Mech. Engrng. **195**, 1573–1593 (2006)
[18] Hauke, G., Doweidar, M.H., Miana, M.: Proper intrinsic scales for a-posteriori multiscale error estimation. Comput. Meth. Appl. Mech. Engrng **195**, 3983–4001 (2006)
[19] Hauke, G., Fuster, D.: Variational multiscale a-posteriori error estimation for quantities of interest. Journal of Applied Mechanics **76**, 021,201(1–6) (2009)
[20] Hauke, G., Fuster, D., Doweidar, M.H.: Variational multiscale a-posteriori error estimation for the multi-dimensional transport equation. Comput. Meth. Appl. Mech. Engrg. **197**, 2701–2718 (2008)
[21] Hauke, G., Fuster, D., Lizarraga, F.: Variational multiscale a-posteriori error estimation for systems: the Euler and Navier-Stokes equations. Comput. Meth. Appl. Mech. Engrg. **(in prep.)** (2013)
[22] Hauke, G., Hughes, T.: A unified approach to compressible and incompressible flows. Comput. Meth. Appl. Mech. Engrg. **113**, 389–395 (1994)
[23] Hauke, G., Hughes, T.: A comparative study of different sets of variables for solving compressible and incompressible flows. Comput. Meth. Appl. Mech. Engrg. **153**, 1–44 (1998)
[24] Hauke, G., Irisarri, D.: Variational multiscale a-posteriori error estimation for systems. Application to linear elasticity. Comput. Meth. Appl. Mech. Engrg. **(in prep.)** (2013)
[25] Hughes, T.: Multiscale phenomena: Green's functions, the Dirichlet-to-Neumann formulation, subgrid scale models, bubbles and the origins of stabilized methods. Comput. Meth. Appl. Mech. Engrng. **127**, 387–401 (1995)
[26] Hughes, T.: The finite element method:Linear static and dynamic finite element analysis. Dover Publications (2000)
[27] Hughes, T., Feijoo, G., Mazzei, L., Quincy, J.: The variational multiscale method: A paradigm for computational mechanics. Comput. Meth. Appl. Mech. Engrg. **166**, 3–24 (1998)
[28] Hughes, T., Sangalli, G.: Variational multiscale analysis: the fine-scale green's function, projection, optimization, localization and stabilized methods. SIAM J. Numer. Anal. **45(2)**, 539–557 (2007)
[29] Larson, M.G., Målqvist, A.: Adaptive variational multiscale methods based on a posteriori error estimation: Energy norm estimates for elliptic problems. Comput. Methods Appl. Mech. Engrg. **196**, 2313–2324 (2007)

[30] Masud, A., Truster, T., L.A.Bergman: A variational multiscale a posteriori error estimation method for mixed form of nearly incompressible elasticity. Comput. Methods Appl. Mech. Engrg. **200**, 3453–3481 (2011)
[31] Verfürth, R.: A posteriori error estimators for the Stokes problem. Numer. Math. **55**, 309–325 (1989)
[32] Verfürth, R.: A posteriori error estimators for convection-diffusion equations. Numer. Math. **80**, 641–663. (1998)
[33] Zienkiewicz, O., Taylor, R.: The finite element method. McGraw Hill (1991)
[34] Zienkiewicz, O.C., Zhu, J.Z.: A simple error estimator in the finite element method. Int. J. Numer. Methods Engrg **24**, 337–357. (1987)

Area de Mecanica de Fluidos, Escuela de Ingenieria y Arquitectura. LIFTEC (CSIC) – Universidad de Zaragoza, C/María de Luna, 3. 50018 Zaragoza, Spain
E-mail: ghauke@unizar.es